

Improving Intervention Efficiency with Downhole X-ray Diagnostics

by Melissa Spannuth, PhD, Senior Physicist, Visuray



Melissa Spannuth
PhD, Senior Physicist
Visuray



Poor well performance and downhole failures have a significant impact on the profitability of a well. To combat this, operators spend billions of USD each year on time-consuming and costly well interventions to improve production and repair hardware. These interventions cover a broad range of activities from straightforward maintenance to complicated workovers, but in all cases, operators strive for efficient and low-risk operations. A major factor contributing to inefficiency in interventions is the lack of reliable information about the current condition of the downhole equipment. When initially planning an intervention, operators frequently infer downhole conditions either from surface measurements or from downhole measurements that are ancillary to the issue they are investigating [1]. Such limited information often fails to accurately diagnose the issue or misses an underlying problem, which in turn leads to ineffectual intervention activities that do not achieve the objectives. The operator must then investigate further using the same insufficient tools and try another intervention. This trial-and-error cycle repeats with costs and non-productive time mounting until eventually the issue is resolved or the operator abandons the original intervention objectives. To break this inefficient cycle, a number of downhole imaging techniques have been developed.

The purpose of downhole imaging is to improve the initial investigation step of the intervention cycle, as well as any subsequent investigations, by providing a clear visual representation of what is happening in the well. Typical techniques include the lead impression block and optical camera, with ultrasonic imaging having been recently introduced. The first technique uses a block of lead lowered inside the well to take an impression of the object [2]. While fast and inexpensive, the impression can often be difficult to interpret. As a second option, optical cameras can provide images in well fluids transparent to visible light or in gas filled wells, but even small traces of oil or particulates will distort the images [3]. As a result, wells must be cleaned and well fluids replaced with clear fluid or gas before attempting optical imaging. A more recent technology involves using ultrasonic imaging to produce an image of an object inside a fluid-filled well [4]. Ultrasonic imaging works even when the well is filled with opaque fluids, but fails when the fluid is too heterogeneous, for example when the fluid contains suspended particles or bubbles, or when the speed of sound is inaccurately estimated.

As an alternative, Visuray has recently introduced the VR90 downhole X-ray diagnostic service [5]. While X-ray imaging has been applied advantageously in the health and security industries for

decades, Visuray is the first company to have successfully adapted this powerful technique to the challenging downhole environment. The primary advantage of using X-rays for imaging in an oil well is that the radiation can penetrate materials that are opaque and highly heterogeneous. Such materials include oil, brine, oil/water mixtures, and fluids with a large amount of suspended particulates, as well as some solid materials such as cement and sediments [6]. The ability of X-rays to “see” in almost any fluid means that the VR90 tool reliably produces accurate diagnoses without extensive well preparation, saving time and money during interventions.

The VR90 tool’s imaging capabilities rest on a patent-pending technique for reconstructing the surface topography of objects in a well based on the X-rays backscattered from the well fluids [6]. The amount of X-ray radiation recorded by the VR90 tool’s detectors depends upon the amount of X-ray-illuminated well fluid between the VR90 tool and the target object in the well. This radiation recorded by each pixel of the detectors is converted into a distance to the surface of the object viewed by that pixel using a semi-empirical formula based on the physics of X-ray scattering. In this way, we reconstruct the surface of the target object in three dimensions.

An example of one such reconstruction is shown in Figure 1 where it is displayed both as a two-dimensional depth map image and a three-dimensional rendering. In the depth map representation, white and light grey pixels represent areas that are closer to the VR90 tool, while black and dark grey pixels represent areas that are farther from the tool (i.e. the depth of the surface of the object is mapped to a grey scale color scheme). The imaging data were obtained during laboratory tests in water made completely opaque by particles of rust suspended in it. The results reveal an easily recognizable adjustable spanner. Fine details on the spanner are visible, such as a small hole in the neck and the threads on the adjustment screw, demonstrating the millimeter-scale resolution of the VR90 tool’s reconstructions. Furthermore, these reconstructions are dimensionally-accurate, so the resulting images and renderings can be used to measure features on the target object with millimeter-scale accuracy. While these results were obtained in the lab, the VR90 service reliably produces the same caliber results in the field – all in real-time without any well preparation necessary.

To demonstrate these capabilities, consider a recent case from offshore Norway [7]. The operator was considering converting the North Sea injector well back into a producer, but the decision on how

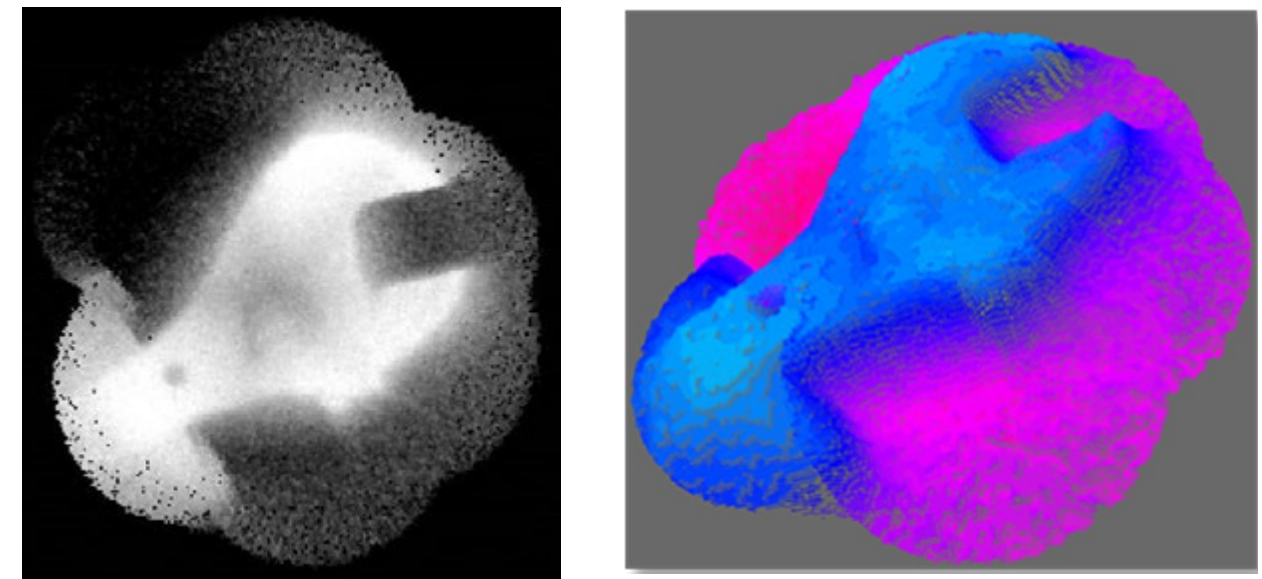


Figure 1. Examples of 2d depth map (left) and 3d rendering (right) from laboratory imaging of an adjustable spanner

to proceed was held up by uncertainty about the downhole safety valve (DHSV). The DHSV had failed during testing and attempts to install an insert DHSV had been unsuccessful. The operator had also attempted to lock the valve open, so they suspected that the flapper on the DHSV was stuck in a partially open position. They wanted to determine whether it would be possible to repair or replace the safety valve as part of the conversion to a producer without having to recompleting the well. Our objectives for the VR90 service’s X-ray diagnosis were thus to investigate the valve and define the clearance through the valve.

We achieved these objectives by acquiring multiple X-ray images with the VR90 tool positioned at various locations within the DHSV. Three of the X-ray images acquired by the VR90 tool are shown in Figure 2. Side view drawings of the corresponding tool and flapper positions, and renderings of what the tool sees are also shown. From top to bottom, the X-ray images show the flapper nearly closed, half-way closed, and almost fully open. As indicated by the drawings, the VR90 tool was resting on the flapper and pushed it open as the tool was moved through the valve. The X-ray images show that the maximum measured opening angle of the flapper was 73°.

In particular, the VR90 diagnostic service provided two key pieces of information: the flapper was not locked open and the flapper could open wide enough to install the insert safety valve. By performing this diagnostic imaging before beginning the intervention on the DHSV, the operator was able to eliminate other time-consuming and risky options, such as recompleting the well or attempting to mill the flapper. Instead, they were able to success-

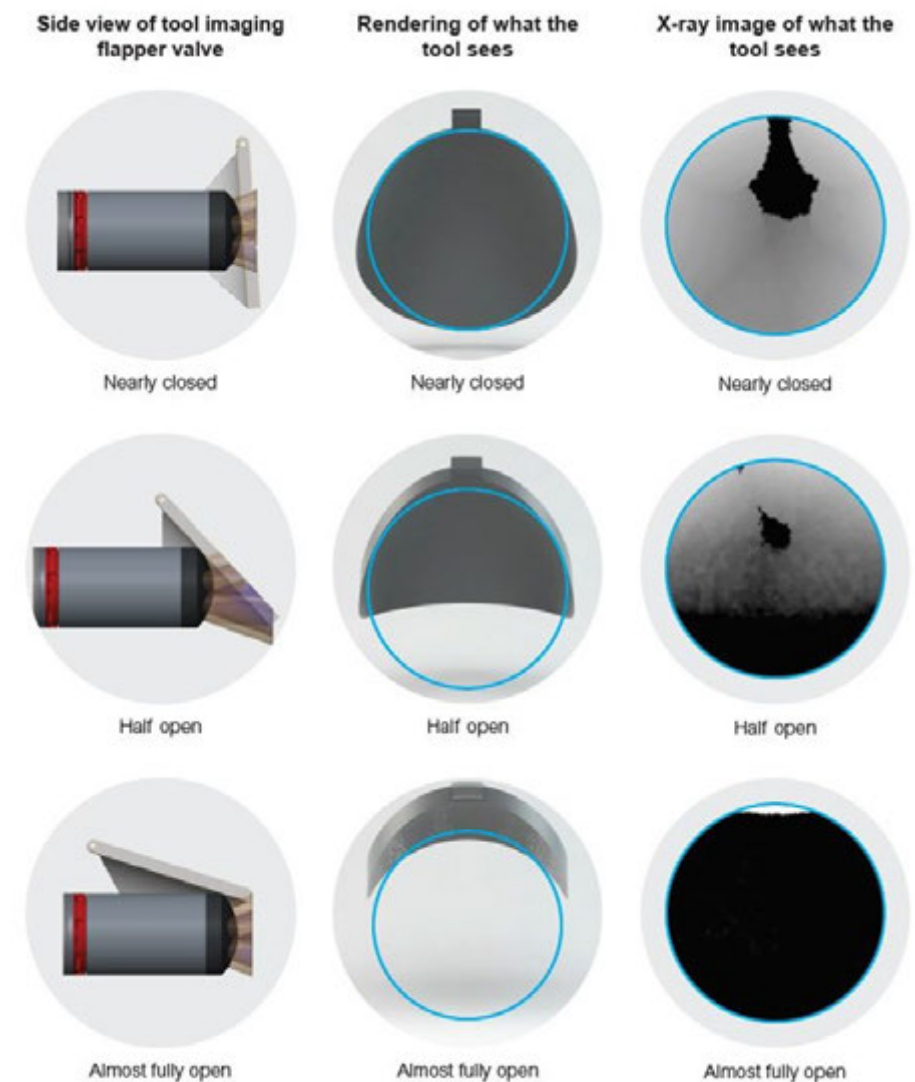


Figure 2. Results of VR90 service’s X-ray investigation of DHSV in a North Sea well

SPE Norway – Well Performance

fully install an insert DHSV, an efficient and cost-effective solution.

In a second example, we provided our service to an operator in the Permian Basin in West Texas. In this case, the tubing was being pulled from the well during an intervention when it became stuck and eventually parted. The remaining tubing needed to be fished, but the fishing company was unsure of the exact location and shape of the top of the fish. The situation was further complicated by the state of the tubing that had been pulled from the well. The bottom of that tubing showed severe damage due to milling, which suggested that the top of the tubing left in hole could be mangled. Our objectives for the VR90 service's X-ray diagnosis were thus to locate the top of the tubing to be fished and provide a visualization of the tubing with accurate dimensions so that the fishing company could design an appropriate fishing tool.

We achieved these objectives by tagging the top of the tubing and then acquiring multiple images above and below the top. One of the resulting images is shown in Figure 3 along with a photograph of the stuck tubing after it was fished from the well. The image reveals that the tubing had been slightly crushed against the casing producing an oval-shape at the top. Additionally, a sharp edge became folded over the top of the tubing blocking the inside of the tubing. The images also revealed damage along the tubing as no clear outer diameter was visible.

Based upon these images, obtained in real-time at the well site, Visuray recommended

against further milling attempts and suggested a specific type of fishing tool. The client chose to follow these recommendations and successfully fished the tubing on the first attempt. When the tubing was pulled from the well, the VR90 service's diagnosis was confirmed as the folded-over top and shredded outer diameter were clearly evident on the fished tubing top. This outstanding outcome was possible due to the dimensional-accuracy of the reconstructions and the quick, reliable results produced by the VR90 service.

Overall, these case studies demonstrate how the VR90 downhole X-ray diagnostic service can be used to improve efficiency in well intervention activities. The VR90 service provides quick, reliable and accurate visualizations of downhole hardware without the need for any well preparation, which makes it ideal as a diagnostic tool. The cases further demonstrate how performing X-ray diagnostics during the early stages of an intervention can turn the typical trial-and-error intervention cycle into an efficient intervention process. Performing intelligent interventions with diagnostic imaging at the outset has the potential to increase intervention efficiency, saving time and money, and reducing the risk associated with well interventions.

[1] McNicol, J. and B. Joppe. 2008. Working Smarter On Well Intervention Operations. Presented at the IADC/SPE Asia Pacific Drilling Technology Conference and Exhibition, Jakarta, 25-27 August. IADC/SPE-115216. <http://dx.doi.org/10.2118/115216-MS>

[2] Walker, G. 1984. Fishing. Presented at the SPE Eastern Regional Meeting, Charleston, 31 October – 2 November. SPE-13360-MS. <http://dx.doi.org/10.2118/13360-MS>

[3] Rademaker, R. et al. 1992. A Coiled-Tubing-Deployed Downhole Video System. Presented at the SPE Annual Technical Conference and Exhibition, Washington D.C., 4-7 October. SPE-24794-MS. <http://dx.doi.org/10.2118/24794-MS>

[4] Hayman, A.J. et al. 1998. Improved Borehole Imaging by Ultrasonics. SPE Prod and Fac 13 (1): 5-14. SPE-28440-PA. <http://dx.doi.org/10.2118/28440-PA>

[5] Teague, P.N. 2011. Imaging of Backscattered Ionizing Radiation – A Key Enabler for through Mud Borehole Imaging. Presented at the Offshore Technology Conference, Houston, 2-5 May. OTC-21667-MS. <http://dx.doi.org/10.4043/21667-MS>

[6] Spannum, M. et al. 2014. X-ray Backscatter Imaging in an Oil Well. Presented at the SPE Annual Technical Conference and Exhibition, Amsterdam, 27-29 October. SPE-170706-MS. <http://dx.doi.org/10.2118/170706-MS>

[7] Spannum, M. et al. 2017. Improving Intervention Efficiency with a Novel X-ray Wireline Diagnostic Service: A Case Study. Presented at the SPE/ICoTA Coiled Tubing and Well Intervention Conference, Houston, 21-22 March. SPE-184798-MS. <https://doi.org/10.2118/184798-MS>

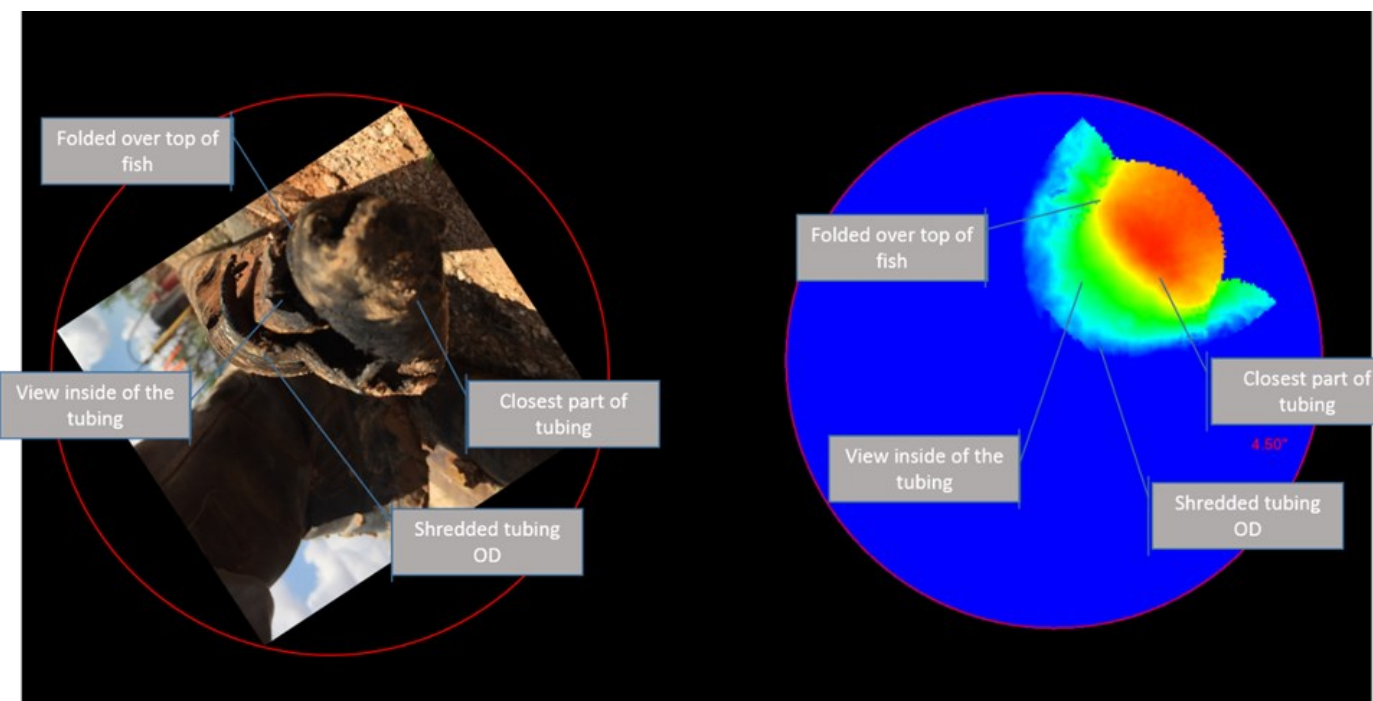
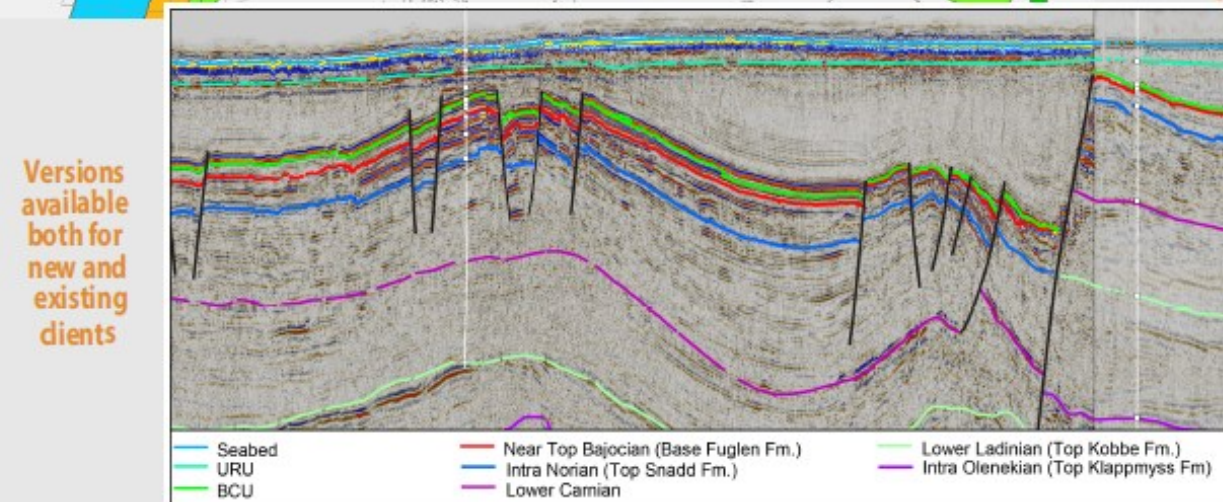
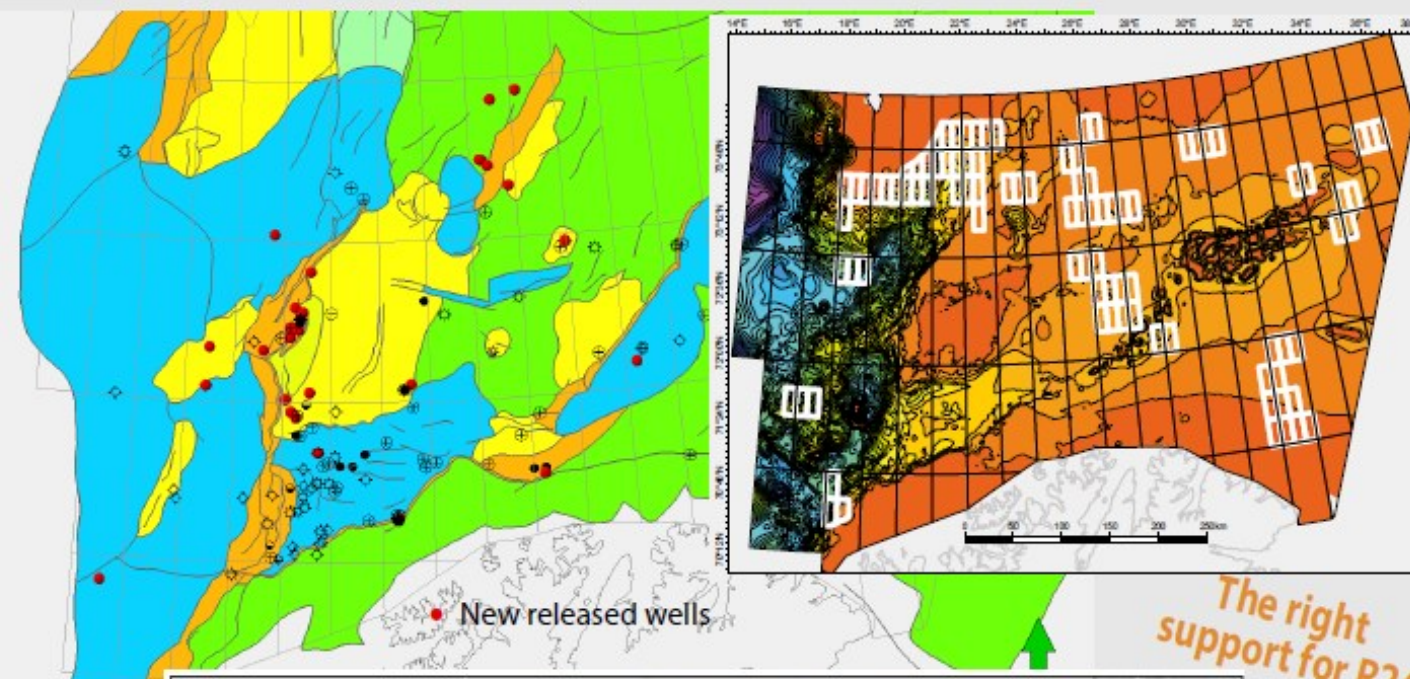


Figure 3. Results of VR90 service's X-ray investigation of parted tubing in Permian Basin (right) and photo of actual tubing pulled from well (left)



Barents Sea Toolkit - 2017 Update



- Petrel project including:**
- All released* wells and well tops
 - Released* 2D and 3D seismic time and phase matched
 - 22 maps from Basement to Seabed merged and covering the entire Norwegian Barents Sea
 - Interpretation and maps updated in light of new data
 - Full petrophysical interpretation of 98 wells
 - Biostratigraphic reanalysis for key wells
 - Velocity model
 - Multiphase and multidisciplinary erosion model
 - Source rock geochemistry and hydrocarbon populations
 - 3D temperature and petroleum system model
 - Hydrocarbon play maps for the entire Barents Sea
- *released before June 2017

